PHYSICAL REVIEW B VOLUME 50, NUMBER 15 15 OCTOBER 1994-I

Electroluminescence study of resonant tunneling in GaAs-AlAs superlattices

R. Klann, H. T. Grahn, and K. Ploog
Paul-Drude-Institut für Festkörperelektronik, Hausvogteiplatz 5-7, D-10117 Berlin, Germany
(Received 31 May 1994; revised manuscript received 13 July 1994)

We have studied the electroluminescence (EL) emission from GaAs-AlAs superlattices embedded in a p^+-i-n^+ diode structure under forward bias. The occupation of higher subbands by sequential resonant tunneling between adjacent wells is demonstrated via interband emission. We observed emission lines due to transitions involving the second and third conduction subband as well as the third heavy-hole subband. The EL lines originating from higher subbands exhibit nearly a constant Stark shift indicating inhomogeneous electric field and carrier density distributions.

I. INTRODUCTION

In two-dimensional systems vertical carrier transport via resonant tunneling leads to a nonthermal occupation of higher electronic subbands as has been reported for coupled multiquantum well, and superlattice, as well as double-barrier structures.[1-3] This effect may be used to design light-emitting devices in the far-infrared spectral region via radiative intersubband transitions.[4-7] Even a population inversion between conduction subbands seems to be achievable in optimized structures offering the possibility for laser operation.[8-11] The relative occupation of the subbands depends strongly on the transfer times between adjacent wells and the intersubband relaxation time. The former vary with the coupling between adjacent wells and can be increased by choosing thin barriers. The intersubband scattering rate depends critically on the subband spacing in comparison with the energy of the longitudinal optical phonons[12] ($\hbar\omega_{\rm LO}$=36 meV for GaAs). To achieve a spacing between the first two electronic subbands below $\hbar\omega_{\rm LO}$, which favors a rather long lifetime in the second conduction subband, the well widths have to be rather large. The resulting intersubband relaxation time is of the order of hundreds of picoseconds[13,14] compared to about less than 1 ps for subband spacings exceeding $\hbar\omega_{\rm LO}$.[1,15-17]

Usually the occupation of excited subbands is studied by photoluminescence spectroscopy. However, in most practical devices the carriers are injected via electric contacts. Therefore, we have realized the electrical injection of carriers by embedding the undoped superlattice in the intrinsic region of a p^+-i-n^+ diode. Furthermore, we have used superlattices with thin barriers in order to achieve short carrier transfer times between adjacent wells. We measure the I-V characteristics and record electroluminescence (EL) spectra in forward bias, i.e., by injecting electrons and holes from the respective contacts into the superlattice. We observe the onset of new EL lines at voltages which coincide with subband tunneling resonances between adjacent wells. Emission due to transitions involving the second and third conduction subband as well as the third heavy-hole subband is identified. The subband resonances lead to an inhomogeneous carrier distribution within the superlattice giving rise to regions with different electric field strengths. These regions are identified by the shift of the band-gap emission line due to the quantum confined Stark effect (QCSE).[18]

Our paper is divided in four sections. In the next section we will summarize the experimental conditions and the sample parameters. In Sec. III we will present theoretical calculations for the sample parameters giving the subband energy levels, the resonant tunneling field strengths, and the oscillator strengths for the corresponding interband transitions. The experimental data of the current-voltage characteristic and the EL spectra are presented in Sec. IV. The experimental results are discussed in Sec. V by comparing the calculations with the experimental data. Finally, a brief summary and conclusion section closes the paper.

II. EXPERIMENT

The investigated sample is a GaAs-AlAs superlattice grown by molecular beam epitaxy on a n^+-(001) GaAs substrate. The 40 periods of a 21 nm wide GaAs well and a 2.2 nm AlAs barrier represent the $\sim$ 1 μm thick intrinsic region of a p^+-i-n^+ diode. The contact layers are heavily doped $Al_{0.5}Ga_{0.5}As$ layers (1×10^{18} cm^{-3}), which are transparent at the emitting wavelengths. Cylindrical diode structures with a diameter of 230 μm are processed out of the wafer by mesa etching techniques. The p^+ region on top is supplied with an ohmic contact using Cr/Au, while the substrate is contacted with AuGe/Ni (n^+ region). The diodes are mounted on the coldfinger of an optical He flow cryostat. All measurements are performed at a temperature of 5 K. The voltage is applied using a Hewlett-Packard (HP) 3245A voltage source. The current is measured with a HP-3458A multimeter. The electroluminescence signal is dispersed in a 1 m grating monochromator. The spectra are recorded using a liquid nitrogen cooled charge-coupled device array.

0163-1829/94/50(15)/11037(8)/$06.00 ©1994 The American Physical Society

III. RESONANCE FIELD STRENGTHS, SUBBAND ENERGIES, AND OSCILLATOR STRENGTHS

To analyze the EL spectra it is important to know the field dependence of the subband energies and, consequently, the interband transition energies involving higher subbands as well as the oscillator strengths of the corresponding transitions. Without an electric field, the situation with regard to the oscillator strength is for infinite barriers very simple, since due to the orthogonality of the wave functions for the different subbands only interband transitions involving the same subband index are allowed. This selection rule breaks down in an applied electric field. At the same time the subband energies, and, consequently, the subband spacings, depend on the electric field strength.

A. Resonance field strengths and subband energies

The resonance field strengths have been numerically calculated by integrating the Schrödinger equation in the envelope function approximation for a coupled double quantum well system in an applied electric field. The resonance field is found by minimizing the level splitting. The results are listed in Table I. Only resonances between the lowest and a higher conduction (valence) subband are shown.

The subband energies are calculated for a single quantum well at the respective resonance fields as determined above and are listed in Table II. The reference energy is the corresponding band edge of bulk GaAs. Excitonic effects are neglected. The conduction subbands are labeled as Cn, while the valence subbands are denoted by Hn for heavy-hole subbands and Ln for light-hole subbands with n denoting the subband index. Note that for zero electric field the spacing of the first two conduction subbands $\Delta E_{C2\text{-}C1}$ is equal to 30.8 meV, which is well below the LO-phonon energy $\hbar\omega_{\mathrm{LO}}$ in GaAs. Furthermore, the heavy-hole subband spacings $H1$-$H2$, $H1$-$H3$, and $H1$-$H4$ as well as the heavy-hole light-hole subband spacing $H1$-$L1$ and $H1$-$L2$ are below $\hbar\omega_{\mathrm{LO}}$(GaAs). The miniband widths of all listed subbands are smaller than 1 meV.

By applying an external voltage V_{ap} to the contacts, the superlattice experiences an electric field F_{ap}, which is determined by the built-in voltage of the p^+-i-n^+ diode (V_{bi}=1.46 V) and the applied voltage. For a homogeneous field distribution it is given by

$$F_{\mathrm{ap}} = \frac{V_{\mathrm{ap}} - V_{\mathrm{bi}}}{L} \quad , \tag{1}$$

where $L = Nd$ is the width of the intrinsic region (N denotes the number of periods and d the superlattice period). With $V_{\mathrm{ap}} = V_{\mathrm{bi}}$ the applied electric field equals zero, i.e., this is the flat-band condition. If V_{ap} exceeds V_{bi}, then electrons are injected from the contact on the substrate side and holes are injected from the top contact. With applied electric field F_{ap} the subband energies shift due to the QCSE.[18] The shift is much larger for carriers with heavier mass, i.e., heavy holes, than for carriers with a light mass, i.e., electrons and light holes. It also depends strongly on the subband index (cf. Table II). The subband spacing is therefore field dependent. The spacing between the first and second electronic subband $\Delta E_{C2\text{-}C1}$ increases with increasing electric field and reaches at 28 kV/cm the LO-phonon energy of GaAs. For even larger electric fields it increases further. This is important since the intersubband relaxation time (τ_{IS}) depends critically on the subband spacing. If the subband spacing is smaller than the LO-phonon energy, a relatively long relaxation time of a few hundred picoseconds for intersubband scattering has been reported.[13,14] For a subband spacing larger than $\hbar\omega_{\mathrm{LO}}$ a short relaxation time of $\tau_{\mathrm{IS}} \leq 1$ ps has been measured.[1,16] This implies that τ_{IS} can change drastically with increasing electric field.

Due to the complicated valence band structure the $H1$-Ln resonance field strengths were not calculated by the procedure described above. However, an estimate of the field strength for resonant tunneling between heavy-hole

TABLE I. Calculated resonance field strengths F_{res} for resonant coupling between the indicated subbands of adjacent wells. The calculation was performed by solving the Schrödinger equation numerically for a double quantum well system in an applied electric field. The applied voltage is calculated from the field strength according to Eq. (1).

Resonant coupling of	F_{res} (kV/cm)	V_{ap}
$H1$-$H2$	2.8	1.74
$H1$-$H3$	4.3	1.89
$C1$-$C2$	13.9	2.85
$H1$-$H4$	15.4	3.0
$H1$-$H5$	25.9	4.0
$C1$-$C3$	39.7	5.43

TABLE II. Calculated subband energies for a single quantum well at selected resonance field strengths of Table I. The energy is given in meV and measured from the corresponding band edge into the respective band. C denotes the conduction band, H the heavy-hole band, and L the light-hole band.

F_{res} (kV/cm)	$C1$	$C2$	$C3$	$H1$	$H2$	$H3$	$H4$	$H5$	$L1$	$L2$	$L3$
0	10.2	41.0	92.6	2	8.1	18.3	32.6	50.9	7.3	29.4	66.3
4.3	10.1	41.1	92.6	1.6	8.3	18.4	32.6	50.9	7.2	29.4	66.3
13.9	9.2	41.4	92.8	-1.8	8.6	19.1	33.1	51.2	5.8	29.8	66.3
39.7	2.2	42.8	94.2	-16.6	3.8	20.6	36.2	53.8	-3.2	31.0	68.6

and light-hole subbands can be obtained using

$$F_{\rm res}^{H1\text{-}Ln} = \frac{\Delta E_{H1\text{-}Ln}}{e\,d} \ , \qquad (2)$$

where e denotes the electron charge. The subband energies of the $H1$ and Ln levels are taken from Table II at zero electric field. The resonances should appear at approximately $F_{\rm res}^{H1\text{-}L1}$=2.3 kV/cm ($V_{ap}$=1.69 V), $F_{\rm res}^{H1\text{-}L2}$=11.8 kV/cm ($V_{ap}$=2.64 V), and $F_{\rm res}^{H1\text{-}L3}$=27.7 kV/cm ($V_{ap}$=4.24 V). The first heavy-hole resonances occur at much lower electric fields than the electronic resonances, because the subband spacings are much smaller. The $H1$-$H4$ resonance appears in the same field range as the $C1$-$C2$ resonance.

B. Oscillator strengths

The intensity I_{ij} for interband emission involving different conduction Ci and valence subbands Hj or Lj is proportional to the product of the occupation numbers n_i and p_j of the respective subbands and to the corresponding oscillator strengths. The oscillator strength of a transition is proportional to the overlap integral O_{ij} of the envelope wave functions $\Phi(x)$

$$I_{ij} \propto n_i \times p_j \times O_{ij} \ , \qquad (3)$$

where the overlap integral is calculated from

$$O_{ij} = \left| \int_{-\infty}^{+\infty} \Phi_i^C(x) \times \Phi_j^{H,L}(x) dx \right|^2 \ . \qquad (4)$$

Taking the envelope wave functions $\Phi_i^C(x)$ and $\Phi_j^{H,L}(x)$ from the numerical solution of Schrödinger's equation, we determine O_{ij} for different subband indices as a function of the applied electric field. The results for the strongest interband transitions (i.e., with largest overlap integral) are shown in Fig. 1. The envelope wave functions are normalized to unity giving a maximum value of 1 for the overlap integral. Note that for vanishing electric field only transitions with equal subband index exhibit a sizable oscillator strength in the investigated samples (e.g., $C1H1$, $C2H2$, etc.). With increasing field O_{C1H1} decreases continuously to about 0.1 for F = 39.7 kV/cm, while the transition probabilities involving higher electronic subbands increase to a maximum value of, e.g. O_{C2H1}=0.6. At the $C1$-$C3$ resonance the $C2H1$, $C3H1$, and $C1H3$ overlap integrals are larger than the one of the $C1H1$ transition. This implies that efficient emission from these transitions can be expected if the involved conduction and valence subbands are significantly occupied. The transitions with equal subband index like $C2H2$ and $C3H3$ are less likely because of the simultaneous low occupation of higher conduction *and* higher valence subbands in the same well and decreasing overlap integrals of the $CnHn$ transitions for larger electric fields. The transitions shown in Fig. 1 are therefore the most probable ones involving a higher subband in one band and the ground state in the other.

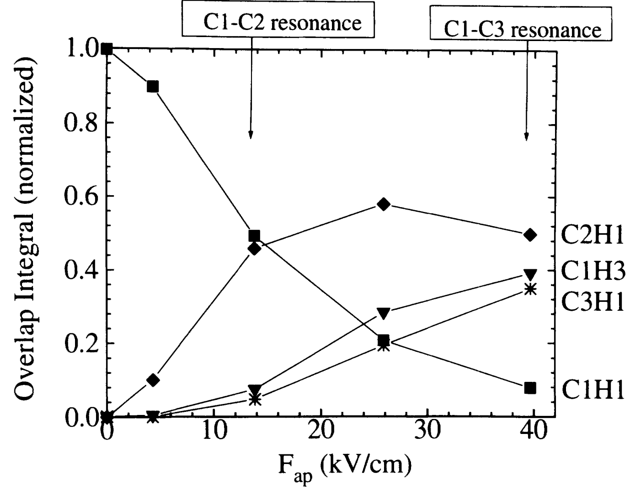

FIG. 1. Overlap integrals of the normalized electron and hole wave functions versus electric field. The involved subbands are indicated. The solid lines are a guide to the eye.

IV. EXPERIMENTAL RESULTS

The dark current-voltage characteristic measured at forward bias is plotted in Fig. 2. For voltages below 3.2 V the current increases continuously. Above 3.2 V we can clearly see three distinct regions exhibiting negative differential conductivity (NDC), i.e., at 3.3, 4.5, and 5.3 V. The data near 5.3 V are shown on an enlarged scale in the inset. The NDC regions are attributed to subband resonances. The current through the superlattice is dependent on the transfer rate of carriers between neighboring wells. A resonant alignment of subbands by

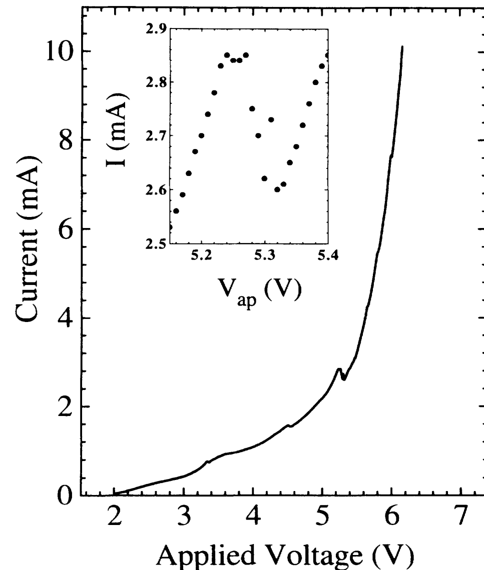

FIG. 2. Current-voltage characteristics in the dark at T = 5 K. The inset shows the region around 5.3 V on an enlarged voltage scale. A current of 1 mA corresponds to a current density of 2.4 A/cm^2.

an appropriate electric field results in fast transfer times by resonant tunneling and therefore allows a high current. Both, an increase or decrease of the electric field strength reduces the current again because the resonance condition is not fulfilled. Electrons as well as holes contribute to the current. We compare the calculated subband resonance voltages with the experimental values to assign the involved subbands. The NDC region at 3.3 V is attributed to the $C1$-$C2$ resonance (calculated value 2.85 V, see Table I). The region at 4.5 V is assigned to the $H1$-$H5$ (cf. Table I) or the $H1$-$L3$ resonance (4.24 V, cf. Sec. III A), while the NDC region at 5.3 V is due to the $C1$-$C3$ resonance (5.43 V). This assignment is based on the I-V characteristic in conjunction with the EL spectra, which are presented in the following.

We have measured the EL spectra in the voltage range from 2.7 to 6.2 V. The emission efficiency (intensity normalized to the current) of the $C1H1$ band-gap transition (1.52 eV) versus photon energy is plotted in Fig. 3. We find a strong emission line for the $C1H1$ transition around 1.524 eV with a double peak structure at low voltages (e.g., 2.7 V). The efficiency decreases with increasing voltage with a resonance maximum at 3.4 V. This maximum coincides with the first NDC region in the I-V characteristic (cf. Fig. 2). For higher voltages (above 3.6 V) the efficiency stays nearly constant on a lower level. The EL-line broadens strongly and splits up into several peaks at lower photon energies. These peaks shift to the red with increasing voltage.

The emission of higher subbands is expected between 20 and 100 meV above the GaAs band gap. The EL efficiency for this photon energy range (1.54 to 1.62 eV) is plotted in Fig. 4. At 2.8 V a new line arises at 1.558 eV having an efficiency maximum at 3.4 V. This line corresponds to the $C2H1$ transition. The linewidth is rather narrow with a full width at half maximum (FWHM) of 3 meV at 3 V. This line is accompanied by two lines of lower intensities, one at higher energy of 1.563 eV ($C2L1$ transition) and the other one at lower energy of 1.546 eV ($C1H3$ transition). For voltages above 3.6 V the efficiency of the main peak saturates. The peak position, however, does not shift with increasing voltage, but remains at the same energy position. Above 6 V the efficiency decreases and the position shifts to lower energies. In this voltage range above 5.4 V a new line emerges at a photon energy of 1.60 eV ($C3H1$ transition). This line is broader than the first one with a FWHM of 8 meV. The strong increase of the background intensity on the low energy side originates from the band-gap transition at 1.52 eV, which is about 200 times more intense (cf. Fig. 3).

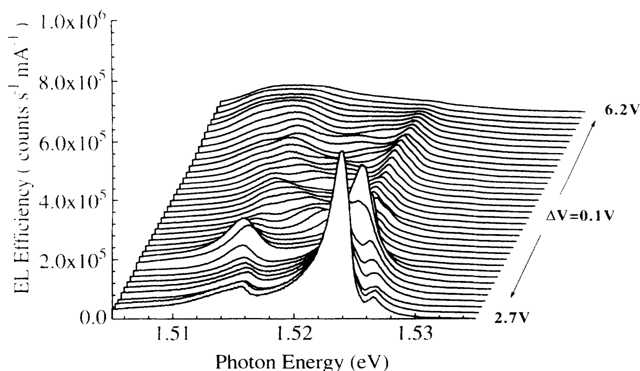

FIG. 3. Electroluminescence efficiency (intensity normalized to the current) of the GaAs-AlAs superlattice vs photon energy in the vicinity of the $C1H1$ transition for applied voltages between 2.7 and 6.2 V in 0.1 V steps at $T = 5$ K.

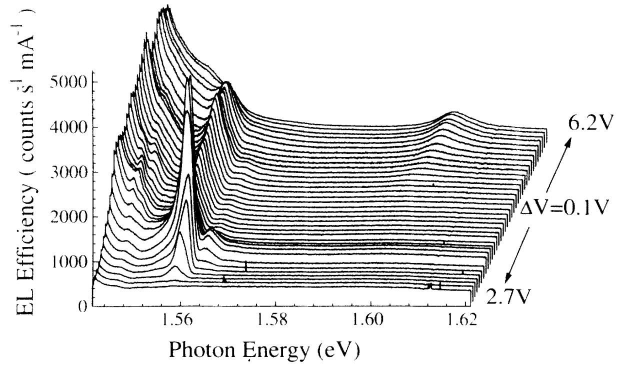

FIG. 4. EL efficiency between 20 and 100 meV above the GaAs band edge for voltages between 2.7 and 6.2 V in steps of 0.1 V. The efficiency is about 200 times less than that of the $C1H1$ transition in Fig. 3.

V. DISCUSSION AND INTERPRETATION

In Fig. 5 the experimentally observed positions of the EL peaks are compared with the calculated energies as a function of the applied voltage. The EL peak positions as derived from Figs. 3 and 4 are shown as dots. The large dots mark the peak positions of the dominating emission lines. The calculated transition energies for the interband emission involving the indicated subbands are shown as solid lines. The energies of the $CiHj$ transitions are calculated as the sum of the Ci-, and Hj-subband energies from Table II plus the energy gap of GaAs (1.52 eV at 5 K). To account for the excitonic binding energy we shift all calculated transition energies by a constant energy value. The shift of a few meV was chosen in such a way that the calculated $C1H1$ transition energy agrees with the experimental value derived from photoluminescence experiments at flatband. We neglect the difference in excitonic energies between different subbands and the shift of the excitonic binding energy with the electric field. The onset of the lines marks the theoretical resonance voltage for the occupation of the higher subband by resonant tunneling from the ground state of the adjacent well. At 2.85 V, for example, the $C1$-$C2$ resonance leads to an occupation of the $C2$ subband resulting in an optical $C2H1$ transition. To compare the applied voltages V_{ap} with the calculated field F_{ap} we assume a linear dependence between V_{ap} and F_{ap} according to Eq. (1), i.e., a homogeneous field distribution.

The assignment of the experimentally observed emission peaks to the calculated subband energies is made by

comparing the emission energies, the resonance voltages, and the expected intensities according to Eqs. (3) and (4). The emission is most intense for interband transitions with the largest value of the overlap integral and highest occupation. We find a good agreement between the energetic position of the main peak at 1.558 eV (large dots) and the calculated $C2H1$ transition energy at 2.8 V. The onset voltage of 2.8 V for the $C2H1$ transition corresponds very well to the calculated $C1$-$C2$ resonance voltage of 2.85 V (cf. Table II). Only above the $C1$-$C2$ resonance an occupation of the $C2$ subband is possible by resonant tunneling resulting in an optical $C2H1$ transition. This is consistent with the calculation of the overlap integral, which shows a significant oscillator strength for the $C2H1$ transition at this field strength. Furthermore, the heavy-hole ground state $H1$ is much more populated than the higher heavy-hole subbands like $H2$ or $H3$. For this reason, the $C2H1$ emission is much more intense than the $C2H2$ line, which is not observed. The less intense line at higher energy is due to the $C2L1$ transition, the $L1$ state being thermally populated. The weak line at 1.546 eV is attributed to the $C1H3$ transition which agrees well with the calculated values. The $C1H2$ transition which is expected to arise 7.4 meV above the $C1H1$ line is not observed in the spectra because the high-energy tail of the $C1H1$ transition is much more efficient than the weak $C1H2$ emission.

We expect for the $C2H1$ transition an increasing redshift with increasing field due to the QCSE (cf. calculated lines in Fig. 5). However, only a constant redshift is observed, i.e., the dominant lines remain at the same energetic position until the $C1$-$C3$ resonance occurs. The EL line from the $C3H1$ transition also seems to exhibit only a constant redshift without a dependence on V_{ap}. The experimental peaks below 1.53 eV lie in the range of the $C1H1$ transition. Instead of an expected single peak shifting strongly to the red with increasing applied voltage according to the QCSE (solid line in Fig. 5), we detect several peaks with the most intense line (large dots) exhibiting no further redshift. However, for voltages above 3.4 V less pronounced broad peaks arise at lower energies

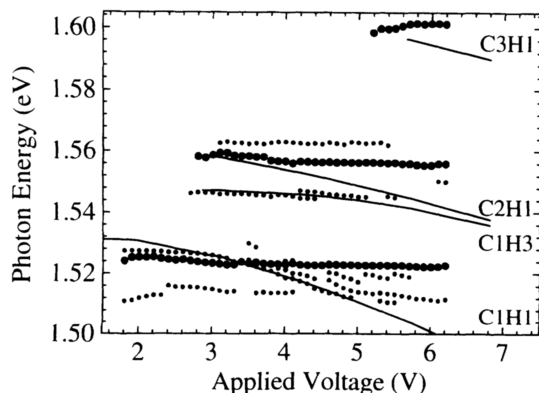

FIG. 5. EL energy peak positions of Figs. 3 and 4 vs applied voltage (dots). The large dots mark the $C1H1$, $C2H1$, and $C3H1$ emission lines (from bottom to top). The solid lines indicate the calculated interband transition energies.

exhibiting a clear redshift.

All these observations demonstrate that the $C1H1$, $C2H1$, and $C3H1$ emission peaks (large dots in Fig. 5) originate from regions of nearly constant electric field within the superlattice in spite of an increasing applied external voltage. The injected carriers are screening the electric field. The field distribution depends on the carrier density and distribution according to Poisson's equation.

For the $C2H1$ transition the Stark-shift remains constant. The emitting wells lie in a region of the superlattice with "pinned" electric field near the $C1$-$C2$ resonance field. For the other parts of the superlattice the field varies with increasing voltage. The $C2H1$ emission originates from this "pinned" region. This is valid for all voltages up to about 6 V. Above that voltage, the $C2H1$ peak shifts to the red and broadens. The $C1H1$ emission stems from the whole width of the superlattice. This means that one part of the emission originates from the region with constant field showing a constant Stark shift. In the other part, the emission should shift further to the red because the field is changing. At the $C1$-$C2$ resonance voltage (3.4 V), which corresponds to the voltage of the maximum intensity of the $C2H1$ emission line, the experimental $C1H1$ peak position (large dots in Fig. 5) coincides with the calculated $C1H1$ transition energy. This is seen in Fig. 5 as a crossing of the calculated $C1H1$ transition line with the experimental large dots at 3.4 V. For voltages above 3.4 V we see the onset of new, lower energetic peaks with increasing redshift for increasing V_{ap} (see Figs. 3 and 5). This results from the inhomogeneous broadening of the $C1H1$ transition due to the different Stark shifts in an inhomogeneous electric field. The wells in the region "pinned" to the $C1$-$C2$ resonance field are emitting with a constant Stark shift according to this field strength (large dots in Fig. 5). The emission of the wells in the other regions, however, shows an increasing red-shift with increasing field. The detected emission is a sum of all wells resulting in a broad peak distribution.

This picture is supported by a calculation of the vertical carrier and electric field distribution. A model with an effective mobility of electrons and holes in the superlattice direction was assumed.[19] Together with Poisson's equation and an effective carrier lifetime of 1.5 ns, we calculated the electron and hole distribution for a given applied voltage. The emission intensity of each well is proportional to the local occupation n times p. The single well peak shifts according to the local field strength by the QCSE. The emission of all 40 wells with a different local electric field according to the calculated field distribution was added up resulting in a broad spectrum. The comparison with the experiment is shown in Fig. 6 for a voltage of 3.8 V (e.g., above the $C1$-$C2$ resonance). The experimental spectrum is indicated as a full line, the calculated spectrum as a dashed line. The intensity is normalized. The peak positions as well as the FWHM are well reproduced. The carrier and field distributions in this voltage range are shown in Ref. 19. For a more precise analysis calculations with an improved model taking into account a field dependent mobility along the super-

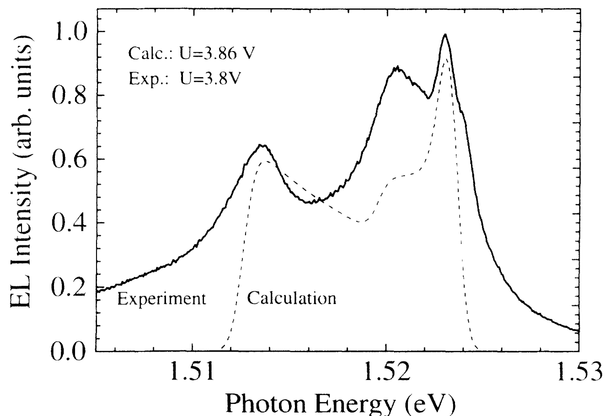

FIG. 6. Experimental EL spectrum of the $C1H1$ transition at 3.8 V (full line) compared with a model calculation (dashed line) taking into account a broadening due to an inhomogeneous electric field distribution.

lattice direction are necessary.

The peak intensities of the $C1H1$, $C2H1$, and $C3H1$ emission lines (large dots in Fig. 5) and the I-V characteristic are shown in Fig. 7. Please note the different scales in efficiency for the three emission lines. We observe distinct features which are correlated to the subband resonances. The onset of the $C1H1$ emission at 1.7 V is connected to hole resonances ($H1$-$L1$ at 1.69 V, $H1$-$H2$ at 1.74 V, $H1$-$H3$ at 1.89 V) which allow an efficient transport of holes from the top contact into the superlattice. The hole resonances are important for an efficient emission because they lead to a sufficient supply

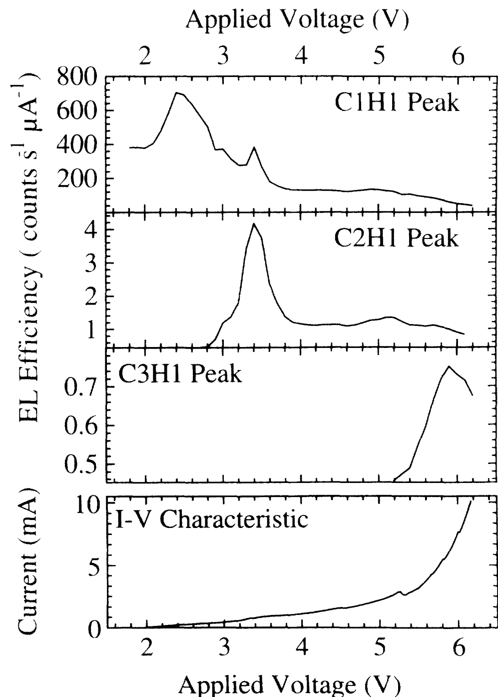

FIG. 7. EL peak efficiency of the $C1H1$, $C2H1$, $C3H1$ emission lines (see Fig. 5) and I-V characteristic vs applied voltage.

of heavy holes into the superlattice region. In the range of the onset voltage of the $C2H1$ emission at 2.8 V a third heavy-hole tunneling resonance occurs ($H1$-$H4$ at 3.0 V). The $C2H1$ efficiency increases to a maximum at 3.4 V. At this voltage a maximum in efficiency is also seen for the $C1H1$ line. The first NDC region in the I-V characteristic occurs also at this voltage. The maximum in emission intensity corresponds to a minimum of the current. The observed resonance value is somewhat higher than the expected voltage of 2.85 V for the $C1$-$C2$ resonance. The reason for this discrepancy is the inhomogeneous field distribution within the superlattice and/or a possible series resistance of the cladding layers.

The occupation of the $C2$ subband can be estimated from the ratio of the $C2H1$ transition to the $C1H1$ transition.

$$\frac{I_2}{I_1} = \frac{n_2}{n_1} \frac{f_2}{f_1}. \tag{5}$$

I_i and f_i are the intensity and the oscillator strength of the $CiH1$ transition, respectively, and n_i the occupation number ($i = 1, 2$). The values of f_i are proportional to the overlap integrals given in Fig. 1. The ratios are independent of the occupation of the heavy-hole ground state $H1$ because the $C1$ and $C2$ electrons recombine with the same heavy-hole state $H1$. Because of the inhomogeneous carrier distribution in the superlattice direction the ratios are different for wells in different regions within the superlattice. This leads to an underestimation of the occupation numbers because only part of the superlattice is in resonance. The emission peak of the $C1H1$ transition, which does not exhibit an increasing Stark shift with increasing voltage, originates from regions with a constant field near the $C2$-$C1$ resonance field (large dots in Fig. 5 at 1.524 eV). This is supported by the observation that the emission energy of this peak remains constant at a value which coincides with the expected redshift for the $C2$-$C1$ resonance field strength. The crossing of the calculated $C1H1$ transition energy with the experimental data occurs at the resonance voltage of 3.4 V. Thus, we conclude that the wells emitting a $C1H1$ line with a constant redshift of that for the $C2H1$ resonance field are located in the same electric field and spatial region as the wells emitting the $C2H1$ line. The comparison of the intensities of this two lines leads to an estimate of the occupation ratio in this resonance region neglecting reabsorption and assuming a constant linewidth.

The peak ratio I_2/I_1 for a voltage of 3.4 V is 0.011 (see Fig. 7). The ratio of the oscillator strengths at the $C1$-$C2$ resonance field is taken from the calculation to be $f_2/f_1 = 0.93$ (Fig. 1). The resulting ratio n_2/n_1 is 0.012. Reabsorption reduces the above band-gap $C2H1$ emission more than the $C1H1$ emission. Taking into account reabsorption the value of n_2/n_1 would be even larger. In the region of the "pinned" $C2$-$C1$ resonance field strength about 1% of the electrons are in the second subband. This demonstrates an efficient occupation of the second subband by resonant tunneling, since at a temperature of $T = 5$ K no thermal population of the second subband is possible.

The $C3H1$ emission intensity peaks at 5.9 V, which

is larger than the calculated value of 5.4 V. Neither the other emission lines nor the I-V characteristic show a resonant behavior at this voltage. For the $C3$ subband the energy spacing with respect to the $C2$ and $C1$ subband is larger than the LO-phonon energy. A fast relaxation to lower subbands via emission of optical phonons can take place. The $C1$-$C3$ resonance leads to a change in the vertical transfer time of electrons resulting in a change of the field distribution. This is seen in the spectra in Fig. 4 at voltages of about 6 V. The $C2H1$ line begins to shift to the red, to broaden, and to decrease in intensity. In the region, which is "pinned" to the $C1$-$C2$ resonance field, the field strength now increases with increasing applied voltage. The same behavior is found for the part of the $C1H1$ line with a Stark shift according to the $C2H1$ resonance field (right peak in Fig. 3).

The estimate of the occupation of the $C3$ subband is more difficult. Because of the large $C3$-$C2$ and $C3$-$C1$ subband spacing one would expect a fast intersubband relaxation out of $C3$. The peak maximum of the $C3H1$ emission is about 18% of that of the $C2H1$ line (see Fig. 7). The $C3H1$ emission originates from regions with a constant field near the $C3$-$C1$ resonance field strength. For the $C2$-$C1$ resonance we used the $C1H1$ line peak at a redshift according to the $C2$-$C1$ resonance field as a reference for the amount of wells at the "pinned" field. In contrast for the $C3$-$C1$ resonance no emission peak energy of the $C1H1$ transition can be identified which is shifted according to the QCSE of the $C3$-$C1$ resonance field. A further difficulty arises from the experimental fact that for voltages near the breakdown voltage (at $\approx$ 6.7 V) the high-energy $C1H1$ emission is more intense than the broad red-shifted $C2H1$ transition. This makes it difficult to observe the $C2H1$ transition for applied voltages above 6.2 V. Therefore, an estimate of the occupation number of the $C3$ subband according to the procedure given for the $C2$ subband is not possible.

The occupation number of the $H3$ heavy hole subband in the region of the "pinned" $C2$-$C1$ resonance field can be given by a similar analysis as for the $C2$ subband. At 3.4 V the ratio of the intensities of the $C1H1$ transition to the $C1H3$ transition is 1000:1 and the ratio of the respective oscillator strengths is 6:1 (cf. Fig. 1). Using Eq. (5) we estimate an occupation of the H3 subband of 0.6% with respect to $H1$. However, because of the more complicated valence band structure and the low intensity of the $C1H3$ transition on the high-energy tail of the $C1H1$ transition this estimation contains a rather large uncertainty compared to the one for the $C2$ subband.

VI. CONCLUSION

We have observed electroluminescence emission from the $C2H1$, $C3H1$, and $C1H3$ interband transitions. The emission lines are identified by calculations of the transition energies, the resonance field strengths and the oscillator strengths, i.e., the overlap integrals of the wave functions. The experimental spectra demonstrate an inhomogeneous field distribution within the superlattice which is determined by electron and hole transport. A nonthermal occupation of the second conduction subband of 1% with respect to the $C1$ subband is found for $C1$-$C2$ resonant tunneling condition. Furthermore, an occupation of the third conduction subband and third heavy-hole subband by resonant tunneling is observed. The transitions involving higher subbands exhibits a constant Stark shift over a wide range of applied voltages indicating a pinning of the electric field within a certain region of the superlattice at the corresponding resonance field strength. A more quantitative description of the inhomogeneous field distribution can be achieved once the model calculation contains the resonant behavior of the drift velocity.

ACKNOWLEDGMENTS

We would like to thank A. Fischer for sample growth and D. Bertram and H. Lage for helpful discussions. This work was supported in part by the European Community ESPRIT Project No. 7193 PARTNERS and the Bundesminister für Forschung und Technologie of the Federal Republic of Germany.

[1] H.T. Grahn, H. Schneider, W.W. Rühle, K. von Klitzing, and K. Ploog, Phys. Rev. Lett. **64**, 2426 (1990).
[2] J.W. Cockburn, P.D. Buckle, M.S. Skolnick, D.M. Whittaker, W.I.E. Tagg, R.A. Hogg, R. Grey, G. Hill, and M.A. Pate, Phys. Rev. B **45**, 13 757 (1992).
[3] D. Bertram, H. Lage, H.T. Grahn, and K. Ploog, Appl. Phys. Lett. **64**, 1012 (1994).
[4] E. Gornik, R. Schwarz, D.C. Tsui, A.C. Gossard, and W. Wiegmann, Solid State Commun. **38**, 541 (1981).
[5] M. Helm, P. England, E. Colas, F. de Rosa, and S.J. Allen, Phys. Rev. Lett. **63**, 74 (1989).
[6] J.W. Bales, K.A. McIntosh, T.C.L.G. Sollner, W.D. Goodhue, and E.R. Brown, in *Quantum-Well and Superlattice Physics III*, edited by G.H Döhler, E.S. Koteles, and J.N. Schulman (SPIE, Bellingham, 1990), p. 74.
[7] J. Faist, F. Capasso, C. Sirtori, D. Sivco, A.L. Hutchinson, S.G. Chu, and A.Y. Cho, Appl. Phys. Lett. **64**, 1144 (1994).
[8] S. Borenstain and J. Katz, Appl. Phys. Lett. **55**, 654 (1989).
[9] R.Q. Yang and J.M. Xu, Appl. Phys. Lett. **59**, 181 (1991).
[10] W.M. Yee, K.A. Shore, and E. Schöll, Appl. Phys. Lett. **63**, 1089 (1993).
[11] J. Faist, F. Capasso, D. Sivco, C. Sirtori, A.L. Hutchinson, and A.Y. Cho, Science **264**, 553 (1994).
[12] P.J. Price, Ann. Phys. **133**, 217 (1981).
[13] D.Y. Oberli, D.R. Wake, M.V. Klein, J. Klem, T. Henderson, and H. Morkoç, Phys. Rev. Lett. **59**, 696 (1987).
[14] J. Faist, C. Sirtori, F. Capasso, L. Pfeiffer, and K.W. West, Appl. Phys. Lett. **64**, 872 (1994).
[15] A. Seilmeier, H.J. Hübner, G. Abstreiter, G. Weimann, and

W. Schlapp, Phys. Rev. Lett. **59**, 1345 (1987).
[16] M.C. Tatham, J.F. Ryan, and C.T. Foxon, Phys. Rev. Lett. **63**, 1637 (1989).
[17] D. Collings, K.L. Schumacher, F. Raksi, H.P. Hughes, and R.T. Phillips, Appl. Phys. Lett. **64**, 889 (1994).
[18] D.A.B. Miller, D.S. Chemla, T.C. Damen, A.C. Gossard, W. Wiegmann, T.H. Wood, and C.A. Burrus, Phys. Rev. Lett. **53**, 2173 (1984).
[19] H.T. Grahn, D. Bertram, H. Lage, K.v. Klitzing, and K. Ploog, Semicond. Sci. Technol. **9**, 537 (1994).